SLURRY FISCHER-TROPSCH/MOBIL TWO-STAGE PROCESS OF CONVERTING SYNGAS TO HIGH-OCTANE GASOLINE. QUARTERLY REPORT, 1 JANUARY-31 MARCH 1981

MOBIL RESEARCH AND DEVELOPMENT CORP.
PAULSBORO, NJ

APR 1981
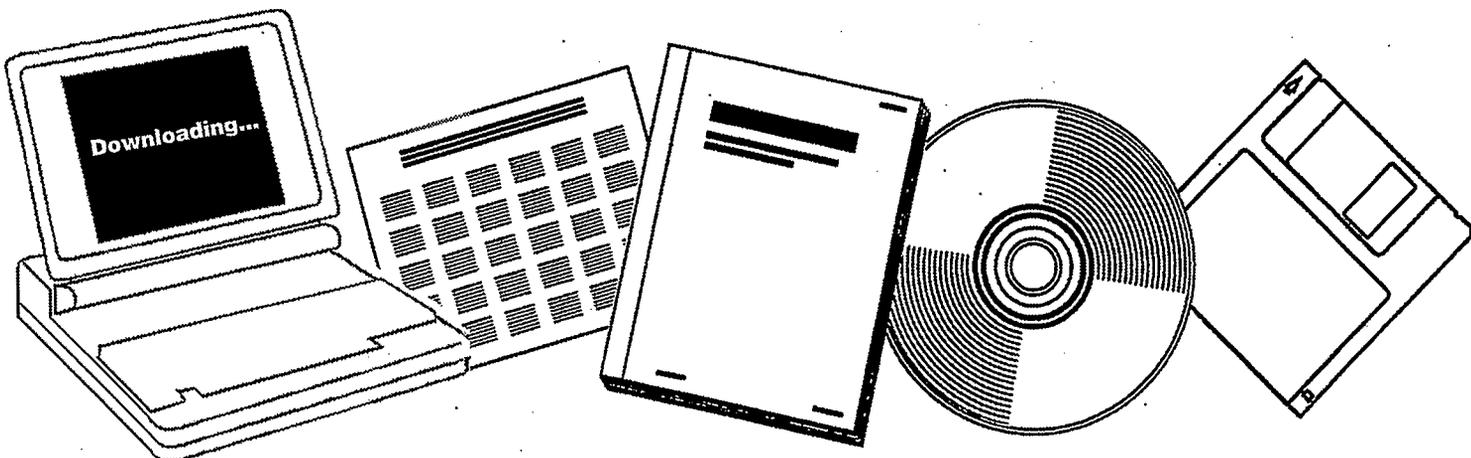
SLURRY FISCHER-TROPSCH/MOBIL TWO-STAGE PROCESS
OF CONVERTING SYNGAS TO HIGH OCTANE GASOLINE

QUARTERLY REPORT FOR THE PERIOD
1 JANUARY - 31 MARCH, 1981

REPORT PREPARED BY: J. C. W. KUO

CONTRIBUTORS: S. K. ADITYA
D. BUKUR
K. M. GUPTE

MOBIL RESEARCH AND DEVELOPMENT CORP.
PAULSBORO, NEW JERSEY 08066

DATE PUBLISHED - APRIL 1981

PREPARED FOR THE UNITED STATES
DEPARTMENT OF ENERGY
UNDER CONTRACT NO. DE-AC22-80PC30022

TABLE OF CONTENTS

I. <u>Abstract</u>

The design phase of the bench-scale pilot plant of the two-stage slurry Fischer-Tropsch/ZSM-5 process has been completed. The shop fabrication phase of the BSU has been initiated, and all major purchasing orders have been issued.

The simple mathematical model of the F-T bubble column reactor has been improved and used to assist the design of the reactor. The kinetic constants required for the mathematical model were estimated using the experimental data from published sources.

II. Objective and Scope of Work

The overall objective of the contract is to develop a two-stage slurry Fischer-Tropsch/ZSM-5 process for direct conversion of syngas, of the type produced in a coal gasification system, to a high octane gasoline. The immediate objective is to design, construct, and operate a bench-scale pilot plant so that the economic potential of this process concept can be evaluated. To accomplish these objectives, the following specific tasks will be undertaken:

Task 1 - Design of Bench-Scale Pilot Plant

A two-stage slurry F-T/ZSM-5 bench-scale pilot plant will be designed for conversion of syngas to high octane gasoline. The slurry F-T reactor will be 2" ID and 25' high. The fixed-bed ZSM-5 reactor will be 2" ID and 4-18" high. A distillation column will be designed to obtain stabilized gasoline products.

Task 2 - Construction and Shakedown of Pilot Plant

The pilot plant will be constructed in MRDC Paulsboro Laboratory. The unit will be shaken down when completed.

Task 3 - Operation of Pilot Plant

At least three slurry F-T catalysts will be tested in the bench-scale pilot plant. At most one of these catalysts may be provided by DOE's alternate catalyst development projects. The best first-stage catalyst together with a ZSM-5 class zeolite catalyst will be used for process variable studies and catalyst aging tests in the bench-scale unit. Products obtained from the unit will be evaluated to define their qualities.

Task 4 - Conceptual Design Study

A preliminary conceptual design of the process will be developed for a commercial size plant for the conversion of syngas to high octane gasoline. Scoping costs of the plant will be estimated.

III. Summary of Progress to Date

The Engineering Flow, and Piping and Instrumentation diagram for the last section of the BSU, the slurry F-T reactor section, is complete. The Detailed Engineering Designs of the major BSU components are also complete. The design of the BSU is now finished although a continuous refinement of the design is expected during the construction phase of the BSU.

The simple mathematical model of the F-T bubble-column reactor has been improved and used to assist the design of the reactor. The kinetic constants which are essential for the model application were estimated using the experimental data of F-T bubble-column reactors from five published sources. A kinetic rate constant of 1.1 mL liquid/s-gFe for precipitated-Fe type catalysts at 268°C is recommended for the current study. This value is substantially smaller than the base value adopted for the parametric studies reported in the last Quarterly Report. These parametric studies have been repeated with this up-dated kinetic rate value and a higher hydrogen diffusivity value estimated from a new liquid-phase diffusivity correlation. The conclusions drawn from these studies are the same as those reported in the last report. The effect on the model prediction of the bubble-column performance due to the changing gas velocity and gas bubble size along the reactor resulting from the molar contraction of the F-T reaction was also evaluated. This effect is small provided an arithmatic mean value of the gas velocities at the reactor inlet and exit is used in calculating the gas hold-up in the model calculation.

IV. **Detailed Description of Technical Progress**

    A. **Task 1 – Design of Bench-Scale Pilot Plant (BSU)**

        1. **Engineering Flow and Piping and Instrumentation Diagrams**

        In the last Quarterly Report, the Bench-Scale Unit (BSU) was divided into four sections:

- Gas feed

- Slurry F-T reactor

- Fixed-bed ZSM-5 reactor and product recovery

- Liquid hydrocarbon product distillation

The Engineering Flow, and Piping and Instrumentation diagrams for all sections, except for the slurry F-T reactor section, were complete in the last quarter and included in that report. The diagram for the slurry F-T reactor section is now also complete (Figure 1) and its description is given below.

        The slurry reactor (2" ID x 25' L) consists of one 5' and two 10' sections of 2"-schedule 40 stainless steel pipe connected together with flange joints. The sectioning of the reactor into 10' and 20' levels offers the flexibility of design modifications if warranted.

        The hot synthesis gas (H_2+CO) from the Feed Pre-heater enters the bottom zone below a distributor, which is clamped between the bottom flanges. A drain is provided in the zone below the distributor to drain any slurry seeping through the distributor.

        At the top, a disengaging zone (5" ID x 6' L) is provided to separate outgoing gases from the gas-liquid suspension. Two inclined baffles are in this zone to break-up any froth formed and to minimize any liquid entrained in the gas. The product vapors leave this zone through a very fine filter which prevents any catalyst carryover.

        A coolant, such as Mobiltherm 600, will be circulated through a jacket surrounding the reactor either to remove the heat of reaction or to add heat as may be required. The cooling jacket is divided into many sections to facilitate the attachment of pipe couplings to the reactor at different levels. These pipe couplings are used for the insertion of different probes (e.g. temperature, pressure, and liquid-level probes) and lines

for the addition or withdrawal of slurry. Four sample taps are provided at 1', 5', 10' and 20' levels to withdraw slurry into sample bombs.

The catalyst slurry is prepared in a 5-gallon Slurry Tank (E-48) and transferred to the reactor above the distributor by applying N_2-pressure in the slurry tank. The Slurry Transfer Vessel (E-49) is used to add small quantities of slurry, if needed, during the operation of the reactor.

In case of accumulation of liquid hydrocarbon products in the reactor, a small amount of the liquid can be withdrawn through a fine filter suspended at a level of approximately 7'. The withdrawn liquid is collected in the Spent-wax Receiver (E-23). The fresh liquid without catalyst is stored in the Fresh-wax Reservoir (E-22). The wax from these two tanks can be pumped into the reactor in the case of a loss of the slurry.

A partial condenser (E-8, Liquid Drop-out Pot) is employed on the product line before the products are sent to the second-stage reactor. If a drop in slurry level occurs within the bubble-column, this condenser can be used to recover some of the heavier hydrocarbons from the F-T reactor effluent and returned it to the F-T reactor.

To analyze first-stage F-T reactor products, a small side-stream can be diverted from the effluent stream. The hot and cold condensers (E-93, 94) separate this sample stream into heavy and light liquid hydrocarbons, aqueous phase, and light gases. These four streams can then be analyzed separately.

2. Detailed Engineering Design of Bench-Scale Pilot Plant Components

The detailed fabrication drawings of most BSU components - Distillation Columns, Pre-heaters, Condensers, Receivers, Drop-out pots, and Glycol flow measuring systems - are complete. Table 1 gives the list of the 40 drawings completed to date. The detailed designs for both the F-T and the ZSM-5 reactors are complete and the preliminary fabrication drawings for the slurry F-T reactor are attached.

The preliminary detail designs of six of the seven sections for the F-T bubble-column reactor are shown in Figures 2 and 3. Figure 2 shows section 1, the top flange with a filter attachment; section 2, the disengager; and section 7, the bottom section below the distributor. Also shown in the drawing is the overall layout of the reactor. Figure 3 shows sections 3, 4, and 5 of the reactor between 20'-25', 10'-20', and 0'-10' levels, respectively. Both figures show cooling jackets and pipe couplings for the insertion of different probes as described in

the previous subsection.

3. Fischer-Tropsch Bubble-Column Mathematical Model and Its Applications

a. Estimation of Kinetic Constants for Slurry Fischer-Tropsch Reactions

Kinetic constants are essential parameters in any slurry F-T reaction mathematical models. Some effort was spent to estimate the constants based on the published experimental data in slurry F-T operations. Data from five sources were used (Koelbel et. al. (1955), Koelbel and Ralek (1980), Schlesinger et. al. (1954), Mitra and Roy (1963), and Kunugi et. al. (1968)). All data were based on bubble-column operations since no data from other slurry reactor types are found.

Since any data from bubble-columns contain both mass transfer and kinetic effects, one must make assumptions to describe the mass transfer phenomenon in order to obtain the kinetic effect. Consequently, the kinetic constants estimated from these data depend strongly on the assumptions used to describe the mass trasnfer phenomnenon. Since all the data, except that from Koelbel et. al. (1955), were obtained from long and slim bubble-columns, it is expected that the effect due to liquid-phase axial dispersion is very small. Therefore, it was decided to use a model of Non-Mixing liquid phase[1] in treating these data. This approach is similar to that used by Deckwer et. al. (1981). Basically the model assumptions are the same as those described in Section IV.3.C of the last Quarterly Report. The formulations of the model follow Deckwer's work exactly and are not repeated here.

The experimental data, all on Fe-base catalysts, from the five sources are summarized in Table 2 and the estimated kinetic constants are given in Table 3. Two types of rate constant expressions are shown below:

$$k_H^{'} = r_H/(1-\epsilon_g)(1-v)C_{HL} \tag{1}$$

$$k_H^{''} = r_H/(1-\epsilon_g)(1-v)C_{HL} \, C_{Fe} \tag{2}$$

Specifically, Expression (2) reflects the loading of the active components, i.e., iron, in the liquid phase, and is a proper one to be used for comparison. Both kinetic expressions were different from the expression, k, used in the last Quarterly

---

[1]Note that we are using "Non-Mixing" to describe the case of axially non-mixing liquid phase instead of the "Plug-Flow" used in the last Quarterly Report. The present name is more descriptive.

Report. That k was defined as

$$k = (1+\beta)r_H/(1-\epsilon_g)C_{HL} \, a_c \tag{3}$$

i.e., a catalytic activity based on the catalyst particle external surface area. Since this k is not an intrinsic kinetic constant, it will no longer be used. The k_H^* is related to k by multiplying the latter with a factor of 5,400 assuming a $\rho_s = 5.2$ g/ml, a $d_c = 2.5$ μm, a $\beta = 1.55$, and a $C_{Fe}/C_{cat} = 0.67$. In Table 3, the kinetic resistances as percentages of the total resistances are also given. These are defined as

$$\frac{R_k}{R_k+R_d} \tag{4}$$

where R_k and R_d are, respectively, the kinetic resistance for H_2 conversion and the H_2 diffusional resistance from the gas-liquid interface to the bulk liquid

$$R_k = K_H/k_H'' \, C_{Fe}(1-\epsilon_g)(1-v) \tag{5}$$

$$R_d = K_H/K_\ell \, a_g \tag{6}$$

In the last Quarterly Report, it was shown that these two are the only important resistances among the five steps attributed to the transfer of H_2 from the gas phase to the catalyst surface and to the H_2 conversion on the catalyst surface.

The same five sets of data were evaluated by Deckwer et. al. (1981) for the kinetic constants. They report k_H' values which are very similar to those reported in Table 3 except that the values from the first two and the last sources are about 7% less than the corresponding values from Deckwer et. al. (1981). This small discrepancy is probably due to some assumptions used in treating the data. They assume that the H_2/CO usage ratio is the same as the inlet H_2/CO ratio and that the H_2 conversion is the same as the H_2+ CO conversion.

By comparing the intrinsic kinetic rate constants, k_H', given in Table 3, the following conslusions can be drawn:

- The catalysts from Koelbel et. al (1955), Koelbel and Ralek (1980), and Mitra and Roy (1963) have catalytic activity within the range 0.85-1.1 mL liquid/s-gFe.

- The catalyst used by Kunugi et. al. (1968) is about 2.3 times more active than those mentioned above.

- The fused-iron catalyst used by Schlesinger et. al. (1954) has a relatively low activity level.

- The kinetic resistance is much larger than the corresponding diffusional resistance provided the gas bubble size is sufficiently small (in this study, $d_B = 0.7$ mm).

Among the five sets of bubble-column data, the first set by Koelbel et. al. (1955) were obtained in a large reactor (1.29 m ID). Since a large reactor may result in a substantial axial dispersion due to the relatively free movement of the liquid, the data must be examined more closely. At the present time, we have not yet built the effect of the liquid phase axial dispersion into the model. For now the Perfectly-Mixed liquid phase model is used. This model was developed in the last Quarterly Report, and the equations can be rearranged as:

$$St_d = -(1+\alpha^*W)^{-1} [\alpha^*X_H^e + (1+\alpha^*Y)\ln(1-X_H^e/Y)] \tag{7}$$

$$St_k = X_H^e/W \tag{8}$$

where
$$St_d = L/u_g^i R_d \qquad St_k = L/u_g^i R_k$$
$$W = C_{Hg}^*/C_{Hg}^i \qquad Y = (1-W)/(1+\alpha^*W)$$
$$\alpha^* = \alpha K$$

Equations (7) and (8) can be solved simultaneously for R_k, the kinetic resistance, which can then be used to estimate k_H' and k_H''. For the data of Koelbel et. al. (1955), they are

$$k_H' = 0.369 \qquad 1/s$$
$$k_H'' = 2.09 \qquad mL \text{ liquid/s-gFe} \tag{9}$$

These rates are about 2.2 times larger than the corresponding values assuming a Non-Mixing liquid phase. This demonstrates that the description of the hydrodynamic behavior will strongly affect the value of the kinetic constants estimated from experimental data from bubble-columns. The actual kinetic values from Koelbel et.al. are probably between the values obtained from the two extreme liquid-phase models, i.e., between 0.93 and 2.1 mL liquid/s-gFe for k_H''. More meaningful values can be obtained after the description of the liquid phase axial dispersion effect is included in the mathematical model.

We recommend that a k_H'' of 1.1 mL liquid/s-gFe at a nominal temperature of 266°C should be used for a precipitated Fe-type catalyst. This value is based on that of Koelbel and Ralek (1980). In the last Quarterly Report, $k_H = 9 \times 10^{-4}$ cm/s

was used. That value is about 4.4 times larger than the present value.

b. Model Applications with Updated Kinetic Constant and Diffusivity Correlation

The study, described in the preceeding sub-section, indicates that the kinetic constant used to predict some bubble-column performances given in the last Quarterly Report was 4.4 times too high. Those calculations are repeated here with the up-dated kinetic rate constant. The values of other model parameters are the same as those given in Table 2 of that report. Nevertheless, a new H_2 diffusivity in the liquid phase is estimated based on a correlation recommended by Satterfield and Huff (1980) and adopted recently by Deckwer et. al. (1981). It is based on H_2 in n-triacontane as predicted by the Wilke-Chang correlation (Satterfield, 1970):

$$D_{HL} = 7.35 \times 10^{-3} \exp(-2285/T) \tag{10}$$

The correlation used in the last Quarterly Report was from Sovova (1976). It gave a value of the H_2 diffusivity about half the one estimated using the current correlation. Generally speaking, the conclusions obtained in the last Quarterly Report remain the same.

Figure 4 shows the effect of kinetic rate and liquid phase mixing on H_2 conversion. It is essential to have a very active catalyst to obtain high conversion within a reasonable reactor height. The liquid phase mixing has a large effect on the required reactor length within the high conversion region. It is expected that the bubble-column reactor in the bench-scale pilot plant will have limited liquid phase mixing and that its performance will fall between the Non-Mixing case and the Perfectly-Mixed case. Nevertheless, unless the catalyst is extremely active, a large reactor height is necessary to achieve high conversion.

Figure 5 shows the effect of molar contraction during the F-T reaction on the H_2 conversion. Only the effect of the molar contraction on the changing reactant concentration is taken into account here. The comparison is with the case assuming no molar change during reaction. The result shows that the reactor height required is about 30% less at high syngas conversion in the case with 50% molar contraction than that with no molar change. It is important to include this effect of molar contraction in the mathematical model.

Figure 6 shows the effect of bubble size on H_2 conversion. Bubble size has a very large effect on column performance. It is extremely important to have small gas

bubbles. The same figure also shows the result of infinite catalytic activity. At infinite catalytic activity, the only resistance to H_2 conversion is the diffusion from the gas-liquid interface to the bulk liquid phase. In other words, this is the best one can do by raising the catalyst conversion activity level. Note that the calculations were done for the Non-Mixing liquid phase case instead of for the Perfectly-Mixed case as given in the last Quarterly Report.

c. Effect of Gas Molar Contraction on Mathematical Model Prediction

Fischer-Tropsch synthesis reaction is accompanied by a decrease in total number of moles. This molar contraction during the reaction will have two effects on the model formulation:

- changing the concentration of the reactants when the conversion increases; and

- changing the hydrodynamic properties, such as the superficial gas velocity, the bubble size, the gas hold-up, and the gas-liquid interfacial area, along the reactor.

The first effect was investigated in the last Quarterly Report. A new calculation was made with an updated kinetic rate constant and a new H_2 liquid-phase diffusivity (Figure 5) of this report. It was concluded that the first effect was important and should be included in the mathematical model. The investigation of the second effect is reported in this subsection.

The effect of the changing hydrodynamic properties along the reactor on the reactor performance is rather complicated. The changing gas-liquid interfacial area (a_g) and gas hold-up (ϵ_g) affect both the gas-liquid interface to bulk-liquid transfer resistance (R_d) and the kinetic resistance (R_k). In order to thoroughly examine this effect, calculations on the following four cases were done:

Cases	u_g in $\epsilon_g=0.053(u_g)^{1.1}$	Bubble Size	Remarks
1	u_g^i	Constant	Present base case (constant ϵ_g and a_g)
2	u_{gm}	Constant	Constant ϵ_g and a_g
3	$u_g(Z)$	Constant	Variable ϵ_g and a_g
4	$u_g(Z)$	Variable	Variable ϵ_g and a_g, but constant number of bubbles

where u_{gm} is the arithmetic average of the inlet and outlet gas

superficial velocities

$$u_{gm} = u_g^i(1 + 0.5\alpha * X_H^c) \tag{11}$$

The gas hold-up (ϵ_g) and the gas-liquid interfacial area (a_g) are related to the gas superficial velocity and the bubble size in the following way:

$$\epsilon_g = 0.053 \ (u_g)^{1.1} \tag{12}$$

$$a_g = 6\epsilon_g/d_B \tag{13}$$

Equation (12) was proposed by Deckwer et. al. (1980).

The equations and the solution for Case 1 were given in the last Quarterly Report (pages 8 and 9). Those for Case 2 are the same as those of Case 1 except that u_{gm} instead of u_g^i is used to evaluate the gas hold-up and the gas-liquid interfacial area. In Cases 3 and 4, both the gas hold-up and the gas-liquid interfacial area vary with the H_2 conversion. An analytical solution is not available. A method of numerical integration, i.e., trapezoidal quadrature, was used to integrate the resulting differential equation. In the Non-Mixing liquid phase case, this differential equation is obtained by combining Equations (3) and (5) of the last Quarterly Report.

Calculations illustrating the effect of variations of hydrodynamic parameters on bubble-column performance are shown in Figure 7 for the case of Non-Mixing liquid phase. For $k_H^u = 1.1$ mL liquid/s-gFe, the differences in model predictions are small and the results for all four cases can be represented by a single curve. For $k_H^u = 4.9$ mL liquid/s-gFe, three curves, corresponding to Cases 1, 2 and 3, are shown in Figure 7. The results obtained for Case 4 fall very close to that of Case 2 and are not shown. Although the deviation between Cases 1 and 3 are quite significant, there is very small deviation between Cases 2 and 3. Consequently, the use of u_{gm} to evaluate the gas hold-up and the gas-liquid interfacial area is sufficient to describe the changing hydrodynamic properties along the reactor resulting from the molar contraction of the F-T reaction.

The effect of the changing hydrodynamic properties on the H_2 conversion in the case of the Perfectly-Mixed liquid phase was evaluated similarly using Equations (7) and (9) of the last Quarterly Report. The differences in results between all four cases are smaller than those between the corresponding cases of the NM Model.

The mathematical model, as illustrated by Case 2, using a constant bubble size and the mean value of the reactor inlet and outlet gas superficial velocities for the calculation of the

gas hold-up, is adequate for catalysts of activity level less than $k_H''=4.9$ mL liquid/s-gFe.

4. Conclusion

The Engineering Flow, and Piping and Instrumentation diagram for the last section of the BSU, the slurry F-T reactor section, is complete. The Detailed Engineering Designs of the major BSU components are also complete. More than forty fabrication drawings are complete, and the shop-fabrication of the liquid hydrocarbon product fractionation column has been initiated. All major purchasing orders for BSU components have also been issued.

The simple mathematical model of the F-T bubble-column reactor has been improved and used to assist the design of the reactor. The kinetic constants which are essential for the model application were estimated using the experimental data of F-T bubble-column reactors from five published sources using Fe-type catalysts. The following conclusions are reached from this study:

- The activity level of the precipitated-Fe catalysts used by Koelbel and Ralek (1980), and Mitra and Roy (1963) are, respectively, 1.1 and 0.85 mL liquid/s-gFe. For the current study, the former value is recommended as a base value for precipitated-Fe type catalysts.

- The activity level of the precipitated-Fe catalyst used by Kunugi et.al. (1968) is about 2.3 times larger than those mentioned above.

- The activity level of the precipitated-Fe catalyst used by Koelbel et.al. (1955) is between 0.93 and 2.1 mL liquid/s-gFe.

- Relative to the four other precipitated catalysts, the activity level of the fused-iron catalyst used by Schlesinger et.al. (1954) is very low.

- For all cases, the kinetic resistance is much larger than the corresponding diffusional resistance, provided the gas bubble size is sufficiently small.

The recommended base value kinetic constant is about 4.4 times smaller than the average kinetic rate constant adopted for the parametric studies reported in the last Quarterly Report. Those parametric studies are repeated here using this up-dated kinetic rate constant value. A new liquid-phase diffusivity correlation is also used. The conclusions obtained in the last Quarterly

Report remain unchanged after these calculations. Evaluations are also done to check the effect on the model prediction of the bubble-column performance due to changing gas velocity and bubble size along the reactor resulting from the molar contraction of the F-T reaction. This effect is small over a wide range of kinetic rate constants, provided an arithmetic mean value of the gas velocities at the reactor inlet and exit is used to evaluate the gas hold-up in the model calculation.

B. Task 2 - Construction and Shakedown of Bench-Scale Pilot Plant

1. Status of the Task

As of this report date, all major equipment -- compressors, pumps, gas meters, heaters, controllers, and vessels -- has been ordered. The other necessary accessories -- valves, fittings etc., -- are also being purchased.

The main fractionation column is being fabricated. The fabrication of other components listed in Table 1 will begin shortly.

2. Conclusion

All major purchasing orders for the BSU equipment are issued. The purchase and the fabrication of the BSU components are on schedule.

3. Future Work

The fabrication of the F-T bubble-column and the ZSM-5 fixed-bed reactor will begin in the next quarter. The fabrication of other BSU components listed in Table 1 will begin shortly.

V. Nomenclature

a_c — Catalyst particle external surface area per slurry volume, $6C_{cat}(1-v)/\rho_c d_c$, (cm^2 solid-liquid area/mL slurry).

a_g — Gas bubble interfacial area, $6\epsilon_g/d_B$, (cm^2 gas-liquid area/mL expanded slurry)

C_{cat} — Catalyst loading, (gCat/mL liquid)

C_{Fe} — Iron loading, (gFe/mL liquid)

C_{Hg} — Gas phase H_2 concentration, (mol/mL gas)

C_{Hg}^* — C_{Hg} in equilibrium with C_{HL}, (mol/mL gas)

C_{HL} — Liquid phase H_2 concentration, (mol/mL liquid)

D_{HL} — Liquid-phase H_2 diffusivity, (cm^2/s)

d_B — Bubble diameter, (cm)

d_c — Catalyst particle diameter, (cm)

d_R — Reactor diameter, (cm)

f — H_2/CO at reactor inlet

K — $f(1+\beta)/(1+f)$

K_H — H_2 solubility coefficient, C_{Hg}^*/C_{HL}, (mL liquid/mL gas)

k' — Synthesis gas conversion rate constant, $(1+\beta)k_H$, (mL liquid/s-(cm^2 solid-liquid area))

k_H — H_2 conversion rate constant, $r_H/(1-\epsilon_g)C_{HL}\,a_c$, (mL liquid/s-($cm^2$ solid-liquid area))

k_H' — Kinetic rate constant for H_2 conversion, $r_H/(1-\epsilon_g)(1-v)C_{HL}$, (1/s)

k_H'' — Intrinsic kinetic rate constant for H_2 conversion, $r_H/(1-\epsilon_g)(1-v)C_{HL}\,C_{Fe}$, (mL liquid/s-gFe)

k_ℓ — Liquid side mass transfer coefficient, (mL liquid/s-(cm^2 gas-liquid area))

L	Bubble column height, (cm)
R_d	H_2 transport resistance from gas-liquid interface to bulk liquid phase, $K_H/k_\ell a_g$, (s-mL expanded slurry/mL gas)
R_k	Kinetic resistance, $K_H/k_H'' C_{Fe}(1-\epsilon_g)(1-v)$, (s-mL expanded slurry/mL gas)
r_H	H_2 conversion rate, (mol/s-mL expanded slurry)
St_d	$L/u_g^i R_d$
St_k	$L/u_g^i R_k$
T	Temperature, (°K)
u_g	Superficial gas velocity, (cm/s)
u_{gm}	$0.5(u_g^i+u_g^e)$, (cm/s)
v	Volumetric fraction of catalysts in slurry, $\rho_L w/(\rho_s+w(\rho_L-\rho_s))$, (mL catalyst/mL slurry)
w	Weight fraction of catalysts in slurry, (gCat/g slurry)
W	c_{Hg}^*/c_{Hg}^i
X_H	H_2 conversion
Y	$(1-W)/(1+\alpha^* W)$
Z	Reactor vertical distance from its entrance, (cm)

Greek Letters

α	Contraction factor, $-\gamma/(1+\beta)$
α^*	αK
β	CO/H_2 mole ratio in F-T reaction
γ	Moles product per mole of H_2 converted in F-T reaction
ϵ_g	Gas hold-up, (mL gas/mL expanded slurry)
ρ_c	Catalyst particle density, (gCat/mL catalyst particle)

ρ_L Liquid density, (g/mL liquid)

ρ_s Catalyst solid density, (gCat/mL catalyst solid)

Superscripts

e   At reactor exit

i   At reactor inlet

I. Literature

Deckwer, W. D., Serpemen, Y., Ralek, M., and Schmidt, B., Chem. Eng. Sci. 36, 765 (1981)

Koelbel, H., Ackerman, P., and Engelhardt, F., Proc. Fourth World Petroleum Congress, Section IV/C, p. 227, Carlo Colombo Publishers, Rome (1955).

Koelbel, H., and Ralek, M., Cat. Rev. Sci. Eng., 21, 225 (1980).

Kunugi, T., Sakai, T., and Negishi, N., Sekiyu Gakkai Shi, 11, 636 (1968).

Mitra, A., and Roy, A., Indian Chemical Engineer, 127 (1963).

Satterfield, C. N. and Huff, G. A., Jr., Chem. Eng. Sci., 35, 195 (1980).

Satterfield, C. N., Mass Transfer in Heterogeneous Catalysis, MIT Press, Cambridge, MA (1970).

Schlesinger, M., Benson, H., Murphy, E., and Storch, H., Ind. Engng. Chem., 46, 1322 (1954).

Sovova, H., Collect. Czech. Chem. Commun., 41, 3715 (1976).

Table 1   Page 18

List of Fabrication Drawings

Drawing Nos.	Description
RB-9074, 9075, 9076	Main Fractionation Column, E-43
RB-9093	Pre-fractionation Column, E-42
RB-9087	Feed Preheater, E-32
RB-9088	Recycle Gas Preheater, E-34
RC-4470	Hot Condenser, E-38
RC-4471	Ambient Water Condenser, E-39
RC-4472	Chilled Glycol Condenser, E-40
RC-4469	Regeneration Gas Condenser, E-35
RD-2694	Inter-reactor Sample (I.R.S) Hot Condenser, E-93
RD-2695	I.R.S. Water Condenser, E-94
RD-2699	Heavy Fuel Oil Vent Condenser, E-100
RE-6229	Wax Drop-out-Pot (Partial Condenser), E-8
RB-9095	Slurry Tank, E-48
RC-4467	Fresh Wax Reservoir, E-22
RC-4468	Spent Wax Receiver, E-23
RC-4473	Heavy Fuel Oil Reservoir, E-41
RC-4474	Two-gallon Distillate Receiver, E-44
RC-4475	One-gallon Distillate Receiver, E-45
RC-4476	Two-gallon Gasoline Receiver, E-46
RC-4477	One-gallon Gasoline Receiver, E-47
RE-6225	Slurry Sample Bombs, E-1, 2, 3, 4
RE-6236	Slurry Transfer Vessel, E-49
RD-2693	H. P. Drop-out Pot, E-26
RE-6234	Water Drop-out Pot, E-29
RE-6240	I.R.S. Hot Condenser Drop-out Pot, E-87

Table 1 (Continued)

RE-6241	I.R.S. Ambient Condenser Drop-out Pot, E-88
RE-6226	Chilled Drop-out Pot, E-5
RE-6227	Surge Pot, E-6
RE-6228	Surge Pot, E-7
RE-6231	Surge Pot, E-17, 18, & 19
RE-6233	Glycol Reservoir, E-24 & 25
RE-6235	Glycol Reservoir, E-30 & 31
RE-6232	Glycol Hold-up Vessel, E-20, 21, 27, & 28
RE-6230	Glycol Overflow Vessel, E-13 & 14
RE-6243	Glycol Overflow Vessel, E-15 & 16
RE-6238	Funnel, E-81, 82, 83, 84, & 96
RE-6239	Funnel, E-97
RE-6237	Gas Mixing Tube, E-55

TABLE 2

Selected F-T Conversion Data in Bubble-Column Reactors

Authors	Catalyst	Temp. (°C)	Pressure (MPa)	Reactor Dimension d_R(cm) x L(cm)	Superficial Inlet Gas Velocity (cm/s)	Inlet H_2/CO	Hydrogen Conversion	H_2/CO Usage Ratio	Catalyst Loading (wt %)
Koelbel et. al. (1955)	Pptd Fe	268	1.2	129 X 770	9.5	0.67	86	0.63	28.4
Koelbel and Ralek, (1980)	Pptd Fe	266	1.1	4.7 X 350	3.5	0.67	85	0.65	15.4
Schlesinger et. al. (1954)	Fused Fe	258	2.17	7.6 X 305	1.54	1.0	63.9	0.81	21.1
Mitra and Roy (1963)	Fe pptd on Kieselgur	260	1.13	5.1 x 305	1.48	1.33	89.7	1.27	17.0
Kunugi et. al. (1968)	Pptd Fe	266	1.12	5.0 X 550	3.78	0.59	80.8	0.59	4.8

TABLE 3

Estimated F-T Kinetic Constants on Fe-catalysts
(Non-Mixing Liquid Phase Model)

Authors	Temperature ($^{\circ}$C)	k_H' (1)	k_H'' (2)	Kinetic Resistance as % of Total Resistance
Koelbel et. al. (1955)	268	0.164	0.931	0.92
Koelbel and Ralek (1980)	266	0.091	1.12	0.80
Schlesinger et. al. (1954)	258	0.024	0.203	0.84
Mitra and Roy (1963)	260	0.055	0.848	0.68
Kunugi et. al. (1968)	266	0.051	2.28	.89

(1) Kinetic rate constant defined as $r_H/(1-\epsilon_g)(1-v)C_{HL}$, (1/s).

(2) Intrinsic kinetic rate constant defined as $r_H/(1-\epsilon_g)(1-v)C_{HL}C_{Fe}$, (mL liquid/s-gFe).

Figure 4

EFFECT OF KINETIC RATE AND LIQUID PHASE MIXING
ON H_2 CONVERSION

H_2 Conversion, (%)

Reactor Height (Ft)

$k_H'' = 2.5$

$k_H'' = 1.1$

$k_H'' = 0.52$ mL Liquid/s-g Fe

- - - NM Model

——— PM Model
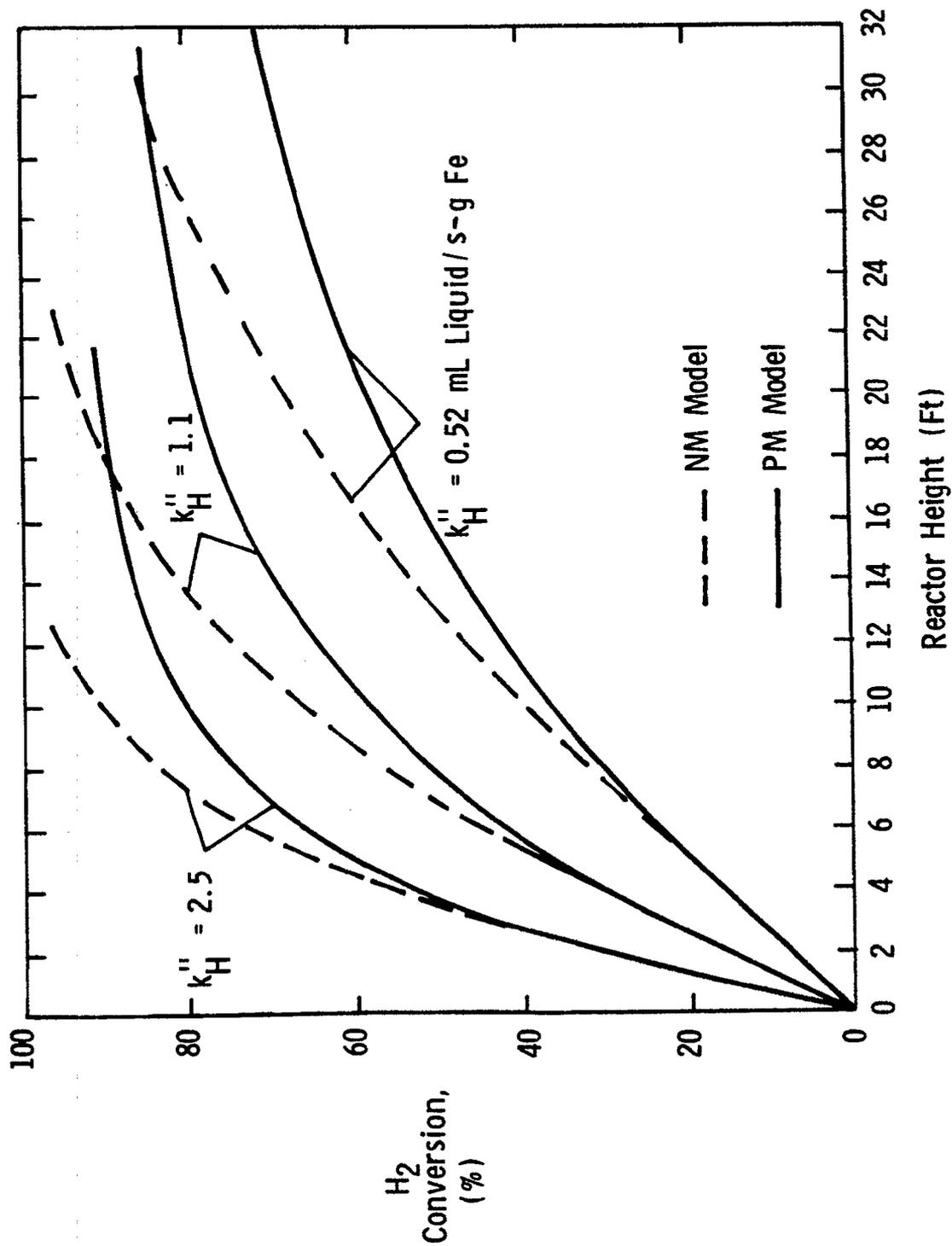
Figure 5

EFFECT OF MOLAR CONTRACTION
DURING REACTION ON H_2 CONVERSION
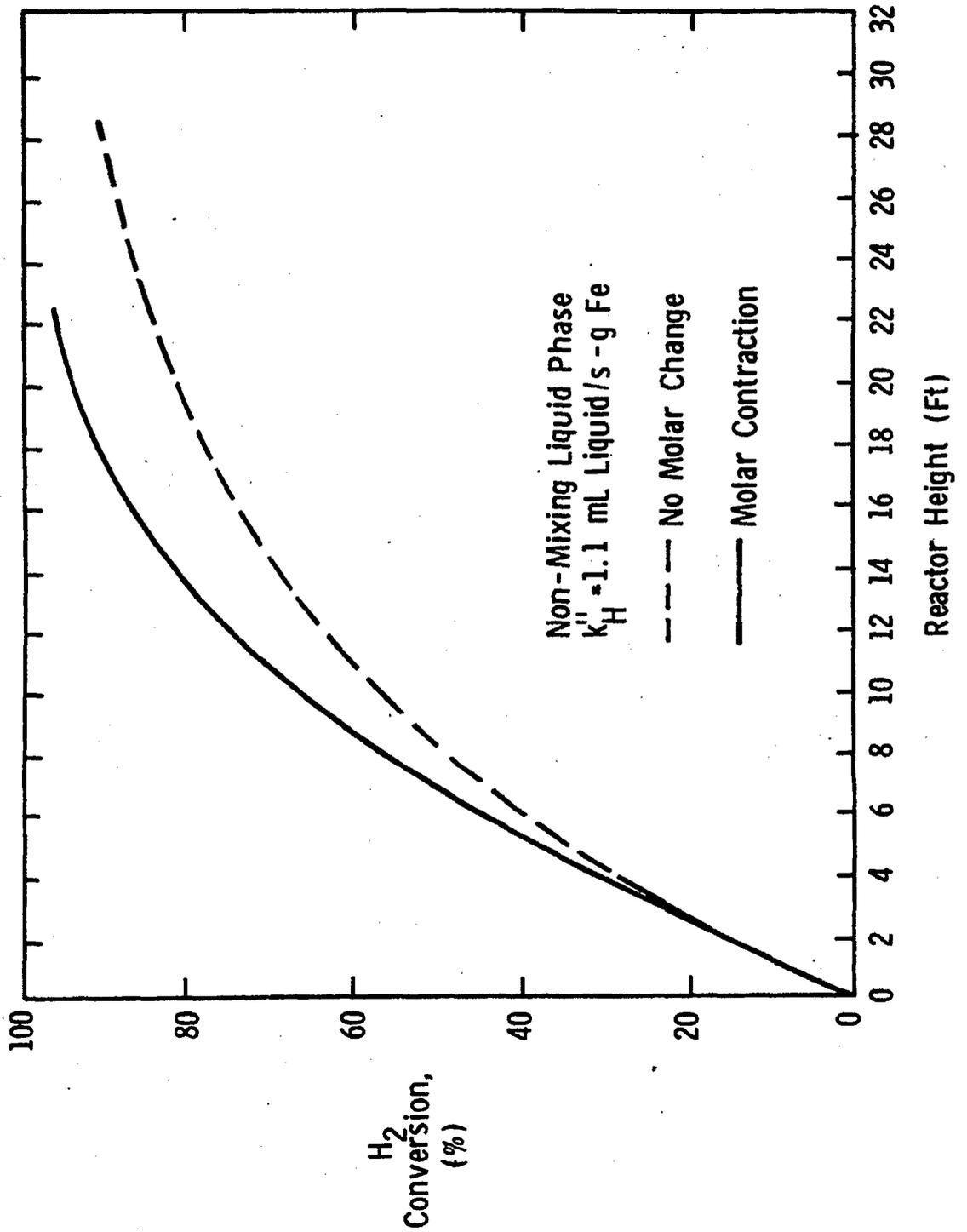
Figure 6

EFFECT OF BUBBLE SIZE ON H₂ CONVERSION

Figure 7

EFFECT OF HYDRODYNAMIC PARAMETERS ON H_2 CONVERSION
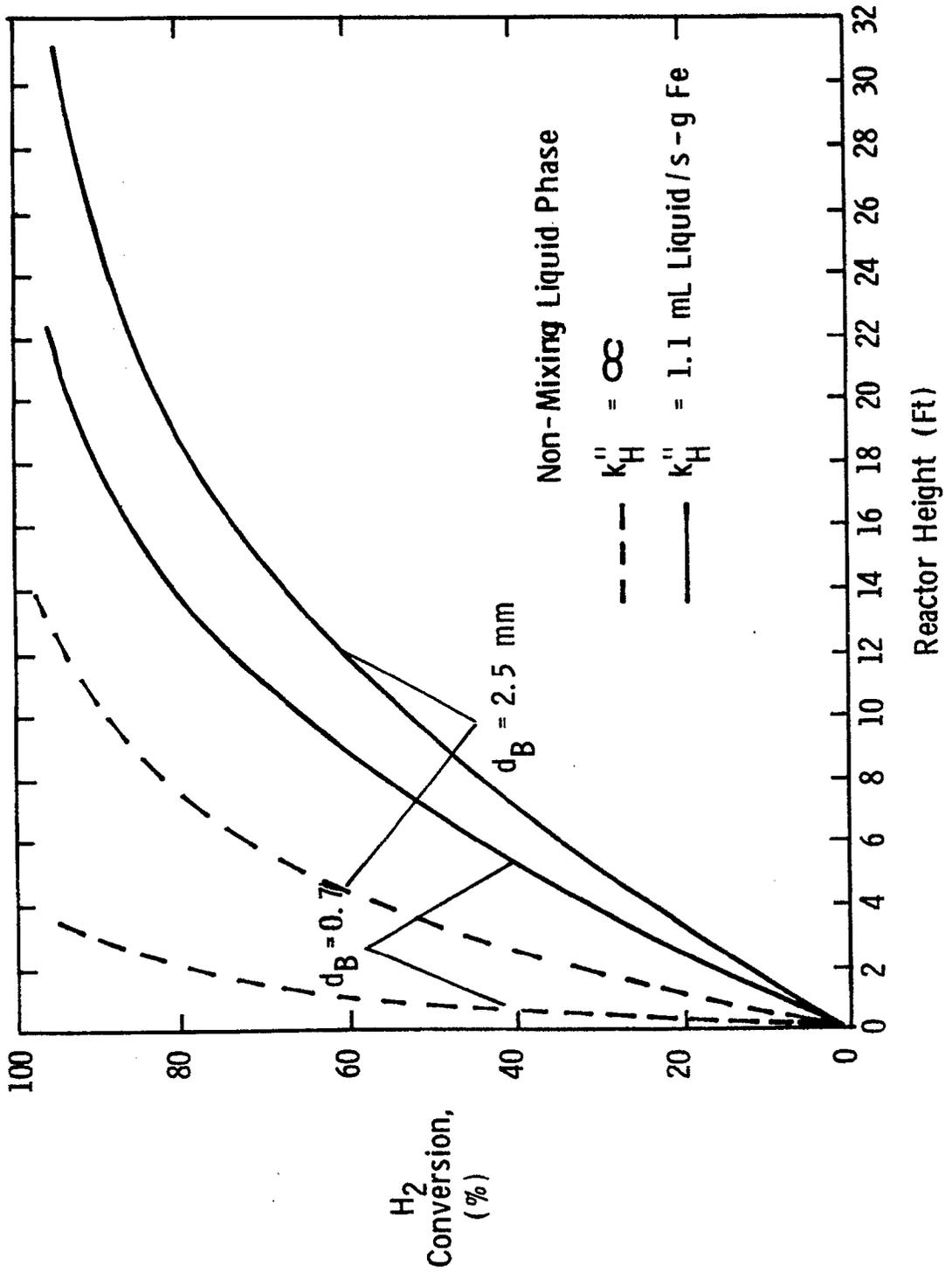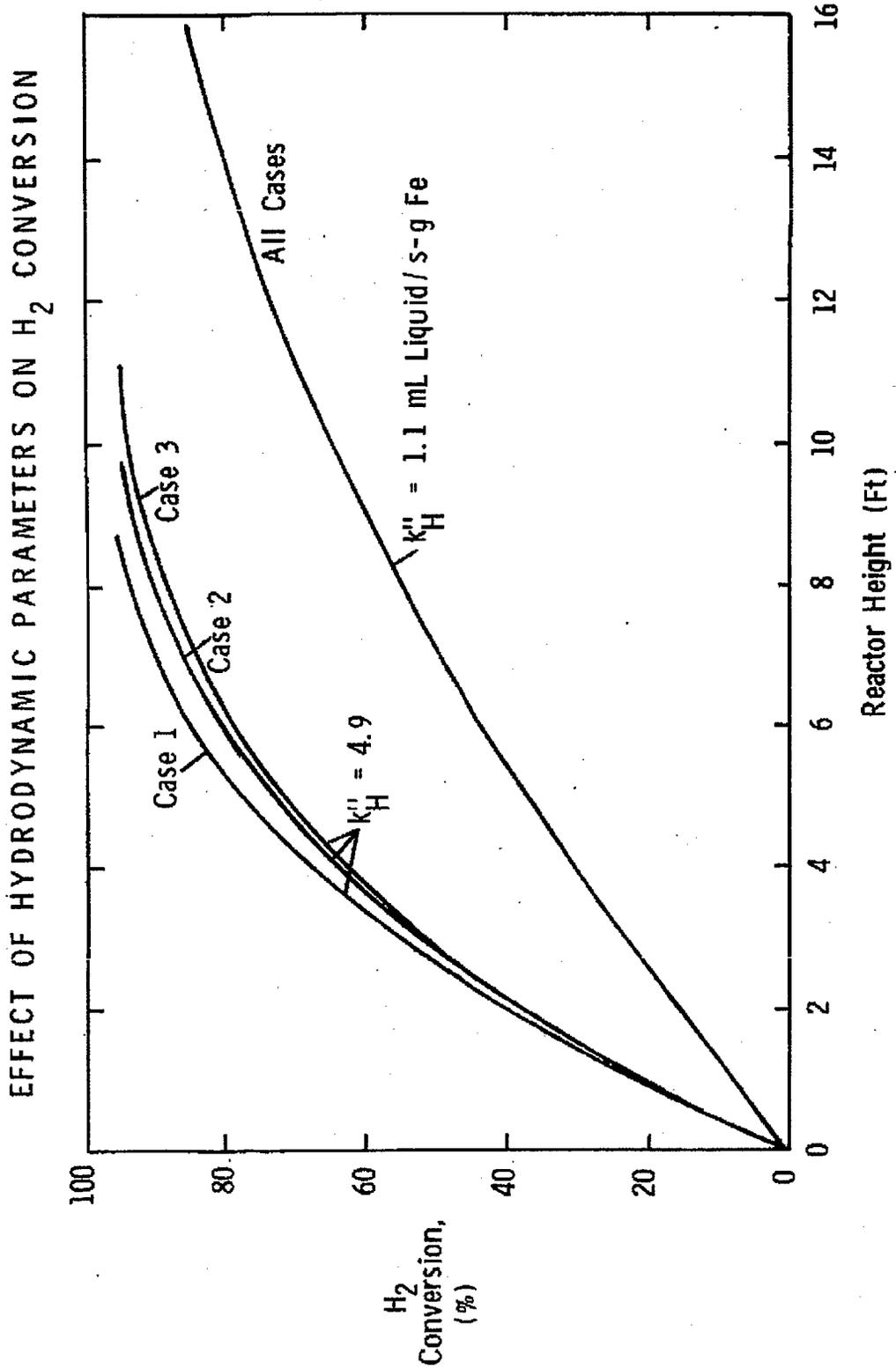
Figure 1
ENGINEERING FLOW, AND PIPING AND
INSTRUMENTATION DIAGRAM:
SLURRY F-T REACTOR SECTION

Figure 2

SLURRY F-T REACTOR
ASSEMBLY AND DETAILS

Figure 3

SLURRY F-T REACTOR
DETAILS